



## MODIS Aerosol Optical Depth Retrievals with high spatial resolution over an Urban Area using the Critical Reflectance

Andréa D. de Almeida Castanho,<sup>1,2</sup> J. Vanderlei Martins,<sup>3</sup> and Paulo Artaxo<sup>2</sup>

Received 3 April 2007; revised 23 August 2007; accepted 30 August 2007; published 16 January 2008.

[1] The retrieval of aerosol optical depth ( $\tau_a$ ) over land by satellite remote sensing is still a challenge when a high spatial resolution is required. This study presents a tool that uses satellite measurements to dynamically identify the aerosol optical model that best represents the optical properties of the aerosol present in the atmosphere. We use aerosol critical reflectance to identify the single scattering albedo of the aerosol layer. Two case studies show that the Sao Paulo region can have different aerosol properties and demonstrates how the dynamic methodology works to identify those differences to obtain a better  $\tau_a$  retrieval. The methodology assigned the high single scattering albedo aerosol model ( $\varpi_o(\lambda = 0.55) = 0.90$ ) to the case where the aerosol source was dominated by biomass burning and the lower  $\varpi_o$  model ( $\varpi_o(\lambda = 0.55) = 0.85$ ) to the case where the local urban aerosol had the dominant influence on the region, as expected. The dynamic methodology was applied using cloud-free data from 2002 to 2005 in order to retrieve  $\tau_a$  with Moderate Resolution Imaging Spectroradiometer (MODIS). These results were compared with collocated data measured by AERONET in Sao Paulo. The comparison shows better results when the dynamic methodology using two aerosol optical models is applied (slope  $1.06 \pm 0.08$  offset  $0.01 \pm 0.02$   $r^2$  0.6) than when a single and fixed aerosol model is used (slope  $1.48 \pm 0.11$  and offset  $-0.03 \pm 0.03$   $r^2$  0.6). In conclusion the dynamical methodology is shown to work well with two aerosol models. Further studies are necessary to evaluate the methodology in other regions and under different conditions.

**Citation:** de Almeida Castanho, A. D., J. Vanderlei Martins, and P. Artaxo (2008), MODIS Aerosol Optical Depth Retrievals with high spatial resolution over an Urban Area using the Critical Reflectance, *J. Geophys. Res.*, 113, D02201, doi:10.1029/2007JD008751.

### 1. Introduction

[2] Air pollution generated in mega-cities has become one of the most important environmental problems in the last few decades because of its hazardous effects on human health and its potential impact on local, regional, and global climate. The development of satellite remote sensing of aerosols over land from the Moderate Resolution Imaging Spectroradiometer (MODIS) has shown a significant potential to enhance air quality monitoring on global and regional scales [King *et al.*, 2003; Chu *et al.*, 2003; Remer *et al.*, 2005]. Nevertheless, major improvements in the accuracy and spatial resolution of the satellite products are still required for air quality applications in urban areas [Li *et al.*, 2005]. The MODIS retrievals provide the total optical depth of aerosol column that depends strongly on the assumed particle microphysical properties (size distribution and spectral refractive indices), as well as on the surface reflectance. Therefore the better the aerosol and surface

optical properties are known, the higher the quality of aerosol retrievals will be. Remer *et al.* [2005] and Chu *et al.* [2003] showed the importance of these variables on the  $\tau_a$  retrieval. Sensitivity studies performed in this paper also show the significance of the accuracy of these input variables.

[3] Sao Paulo is one of the biggest cities in the world, after Tokyo and Mexico City. The population in the Sao Paulo metropolitan area is roughly 20 million ([http://www.ibge.gov.br/home/estatistica/populacao/default\\_censo\\_2000.shtm](http://www.ibge.gov.br/home/estatistica/populacao/default_censo_2000.shtm)). It is located in southeast Brazil on a plateau 860 m above sea level. The annual average  $PM_{10}$  concentration in São Paulo is  $48 \mu\text{gm}^{-3}$ , slightly below the annual average  $PM_{10}$  air quality standard of  $50 \mu\text{gm}^{-3}$ . However, Sao Paulo's  $PM_{10}$  concentrations frequently exceed the daily average of  $150 \mu\text{gm}^{-3}$  during winter when the meteorological conditions are unfavorable to the dispersion of these pollutants, according to data from the local Environmental Protection Agency (CETESB) ([http://www.cetesb.sp.gov.br/Ar/ar\\_geral.asp](http://www.cetesb.sp.gov.br/Ar/ar_geral.asp)). The main sources of aerosols in the region are vehicle emissions, re-suspension of soil dust, and industry [Castanho and Artaxo, 2001]. During the dry season in Amazonia (September, October), the biomass burning plume is transported over long distances and can influence Sao Paulo at its higher altitude [Freitas *et al.*, 2005; Artaxo *et al.*, 2002]. The single scattering albedo ( $\varpi_o$ ) can vary over a wide range, especially when biomass burning aerosol is

<sup>1</sup>Massachusetts Institute of Technology, USA.

<sup>2</sup>University of São Paulo, Brazil.

<sup>3</sup>JCET, University of Maryland Baltimore County, and NASA/Goddard Space Flight Center, USA.

**Table 1.** Deviation of the Retrieved  $\tau_a$  for an Uncertainty of 0.10 in Single Scattering Albedo at 0.55  $\mu\text{m}$  ( $\varpi_o(0.55)$ ), an Uncertainty of 0.05 in Asymmetry Parameter at 0.55  $\mu\text{m}$  ( $g(0.55)$ ) and a 10% Perturbation in Surface Reflectance at 0.65  $\mu\text{m}$  ( $\rho_{\text{surf}}(0.65)$ ) for Different Surface Reflectances at 2.1  $\mu\text{m}$

		Surface Reflectance 2.1 $\mu\text{m}$			
		0.05	0.10	0.15	0.2
		Deviation in $\tau_a$ (%)			
$\varpi_o(0.55) = 0.85 \pm 0.10$	$\tau_{a0.55} = 0.2$	20 %	35 %	60 %	>100 %
	$\tau_{a0.55} = 0.5$	25 %	40 %	60 %	>100 %
$g(0.55) = 0.62 \pm 0.05$	$\tau_{a0.55} = 0.2$	11 %	13 %	15 %	20 %
	$\tau_{a0.55} = 0.5$	13 %	14 %	16 %	21 %
$\rho_{\text{surf}}(0.65) \pm 10\% * \rho_{\text{surf}}(0.65)$	$\tau_{a0.55} = 0.2$	15 %	35 %	65 %	>100 %
	$\tau_{a0.55} = 0.5$	5 %	10 %	20 %	40 %

present. This large variability makes the retrieval of aerosol optical depth with MODIS a challenge since aerosol optical properties can change on timescales of hours to days.

[4] This study presents a tool to identify in an interactive and dynamic way the range of  $\varpi_o$  that better represents aerosols at a specific place and time. We use an aerosol property called the critical reflectance, which is defined in previous work [Fraser and Kaufman, 1985; Kaufman, 1987; Martins, 1999]. This procedure is a step forward from the presumption of a fixed aerosol model and has the advantage of producing a more accurate retrieval of the aerosol optical depth. Surface reflectance is also an important issue and will be discussed. Aerosol optical properties were obtained from climatological analyses of data from AERONET sun-sky radiometer. The retrieved aerosol optical depth with 1.5 km resolution from MODIS using this methodology is compared with AERONET  $\tau_a$  measured from the ground.

## 2. Instrumentation and Database Acquisition

[5] The Moderate Resolution Imaging Spectroradiometer (MODIS) sensor aboard the Terra and Aqua satellites [King et al., 2003; Parkinson, 2003] has provided valuable data since 2000 and 2002, respectively. In this work we used MODIS Level 1B (Collection 4) calibrated and geolocated reflectances (0.65 and 2.1  $\mu\text{m}$ ) with 500 m spatial resolution. The reflectances were used to retrieve the aerosol optical depth with a final spatial resolution of 1.5 km. We also used the standard aerosol optical depth with a spatial resolution of  $10 \times 10$  km from MODIS Level 2 (Collection 5) for qualitative comparison [Remer et al., 2005]. Levy et al. [2007] presents a detailed description of the current MODIS aerosol algorithms and its retrieval accuracy. The Level 1B and Level 2 data were provided by the Goddard Distributed Active Archive Center (DAAC) ([http://daac.gsfc.nasa.gov/data/data\\_set/](http://daac.gsfc.nasa.gov/data/data_set/)).

[6] AERONET is a global ground-based network of sun/sky automated radiometers (CIMEL Eletronique 318A, France) supported by NASA's Earth Observing System (EOS) and other international institutions [Holben et al., 2001]. The Sao Paulo AERONET station has been operating continuously at the University of São Paulo since 2001. This work uses the Sao Paulo AERONET data from 2002 to 2005. Besides  $\tau_a$ , AERONET data also provided the aerosol optical properties [Dubovik and King, 2000] that were used

to define the aerosol optical models (single scattering albedo ( $\varpi_o$ ), asymmetry parameter ( $g$ ) and extinction efficiency ( $Q_{\text{ext}}$ )). The aerosol models defined based on AERONET measurements are appropriate for satellite applications because they represent ambient-condition total column aerosol particles as observed by the satellite, with minimal or no sampling artifacts.

## 3. Sensitivity Tests on the Retrieval of Aerosol Optical Depth From Space Over Land

[7] Sensitivity studies show the importance of the assumed surface reflectance and aerosol optical properties in the retrieval of  $\tau_a$ . The sensitivity of  $\tau_a$  retrieval increases as a function of the surface reflectance. The São Paulo urban area has surface reflectances, ranging from 0.1 to 0.2 at 2.1  $\mu\text{m}$  wavelength, close to the acceptable limit in the standard MODIS aerosol retrieval algorithm over land  $\rho$  (2.1  $\mu\text{m}$ )  $< 0.25$  [King et al., 2003; Remer et al., 2005; Levy et al., 2007]. Our sensitivity analysis (Table 1) shows that an error of  $\pm 10\%$  in a surface reflectance of 0.15 at 2.1  $\mu\text{m}$  wavelength can induce an error of up to 65% in  $\tau_a$ , when  $\tau_a$  is around 0.2. Sensitivity to the surface reflectance is less important for higher  $\tau_a$  values, for example, the difference drops to 20% for a  $\tau_a$  around 0.5, as shown in Table 1. Therefore the higher the  $\tau_a$ , the lower the sensitivity of the  $\tau_a$  retrieval to the surface reflectance assumption. Table 1 also presents the sensitivity of the  $\tau_a$  retrieval to the aerosol model. An error of 0.10 in a single scattering albedo of 0.85, for a mean surface reflectance of 0.15 at 2.1  $\mu\text{m}$  wavelength can induce an error in the retrieved  $\tau_a$  of up to 60%. In Sao Paulo the aerosol single scattering albedo varies from 0.75 up to 0.96. This shows the importance of using accurate information for the single scattering albedo property of the aerosol. The asymmetry parameter typically varies in Sao Paulo from 0.57 to 0.67 at 550  $\mu\text{m}$ . An error of 0.05 in the mean value of  $g(0.55) = 0.62$  can induce an error of around 15% in the  $\tau_a$  retrieved for a surface reflectance of 0.15 at 2.1  $\mu\text{m}$ . The asymmetry parameter is also an important property in the retrieval of  $\tau_a$ , but considering the maximum observed variability in the region is much smaller, its effect is less significant than the single scattering albedo.

[8] The sensitivity test results show the importance of accurate information for the surface reflectance and aerosol optical properties in the satellite retrieval of  $\tau_a$ . The single scattering albedo is the most important aerosol property in

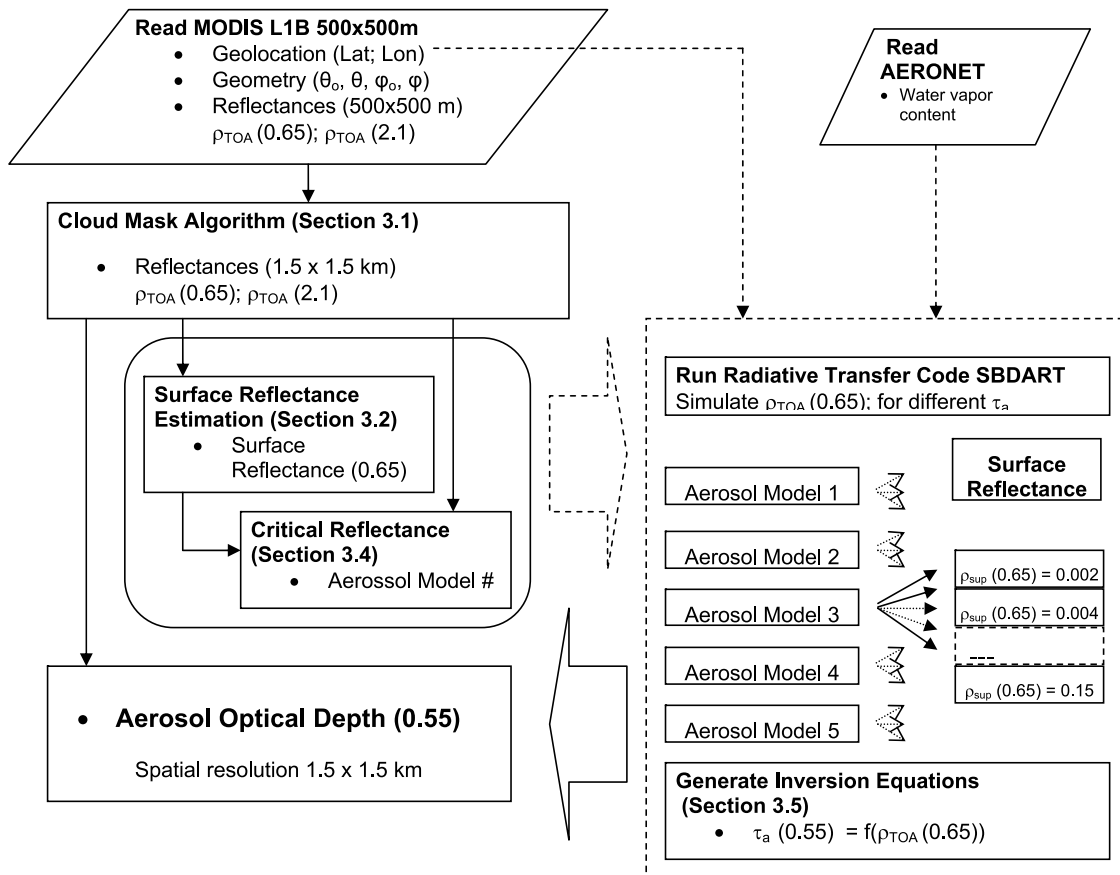


**Figure 1.** Flowchart describing the retrieval of the aerosol optical depth using the critical reflectance determined with satellite measurements.

the retrieval due to its large local variability, and we use this parameter to define the main aerosol models for the region.

#### 4. Retrieving Aerosol Optical Depth From the MODIS Satellite Sensor

[9] In this approach we propose to retrieve  $\tau_a$  with 1.5 km spatial resolution based on MODIS Level 1B calibrated reflectances at 0.65 and 2.1  $\mu\text{m}$ , with a nominal resolution of 500 m at nadir. The 2.1  $\mu\text{m}$  reflectance at the top of the atmosphere (TOA) is used to estimate the surface reflectance at 0.65  $\mu\text{m}$  as described by *Kaufman et al.* [1997a, 2002]. The aerosol optical model used in each  $\tau_a$  retrieval is defined using a dynamic methodology proposed in this work based on the aerosol critical reflectance [Fraser and Kaufman, 1985; Kaufman, 1987; Martins, 1999], which will be discussed in detail hereafter. The use of the critical reflectance in the real time identification of the aerosol model is the main improvement of this study as compared to the MODIS operational algorithm. The retrieval is based on a lookup equation (polynomial function of degree 3) that relates the reflectance at the top of the atmosphere (0.65  $\mu\text{m}$ ) to an aerosol optical depth (0.55  $\mu\text{m}$ ), for a given surface reflectance, aerosol optical model, and satellite and solar geometry. All the equations were generated based on several simulations using the radiative transfer code the Santa Barbara Distort Radiative Transfer Code (SBDART) [Ricchiuzzi et al., 1998]. The flowchart presented in

Figure 1 summarizes the process of computation of the AOD.

##### 4.1. Quality Assurance of the Reflectance at the Top of the Atmosphere

[10] A cloud mask was applied to the MODIS 500 m resolution reflectance data, in a similar procedure as described by *Martins et al.* [2002]. We computed the standard deviation of the reflectance at 0.47  $\mu\text{m}$  of each group of  $3 \times 3$  pixels and discarded the groups that had standard deviations larger than 0.01. To avoid overly dark or bright pixels due to cloud remnants, shadows, or bright surfaces, we also discarded pixels with measured reflectance at 2.1  $\mu\text{m}$  smaller than 0.01 and larger than 0.24, as is also done in the MODIS operational product [Remer et al., 2005; Levy et al., 2007]. For each  $3 \times 3$  set of pixels, we discard the darkest and 4 brightest pixels. The remaining pixels (500 m resolution) were averaged, resulting in a reflectance averaged in a 1.5 km resolution box.

##### 4.2. Estimation of the Surface Reflectance at 0.65 $\mu\text{m}$

[11] The aerosol layer can be considered transparent to the mid-infrared range, allowing the surface reflectance measurement at this wavelength when there is low coarse mode loading. The surface reflectance at 0.65  $\mu\text{m}$  can be estimated using an empirical relationship between the visible (0.65  $\mu\text{m}$ ) and the mid-infrared (2.1  $\mu\text{m}$ ) measurements, as described by *Kaufman et al.* [1997c]. Comparing

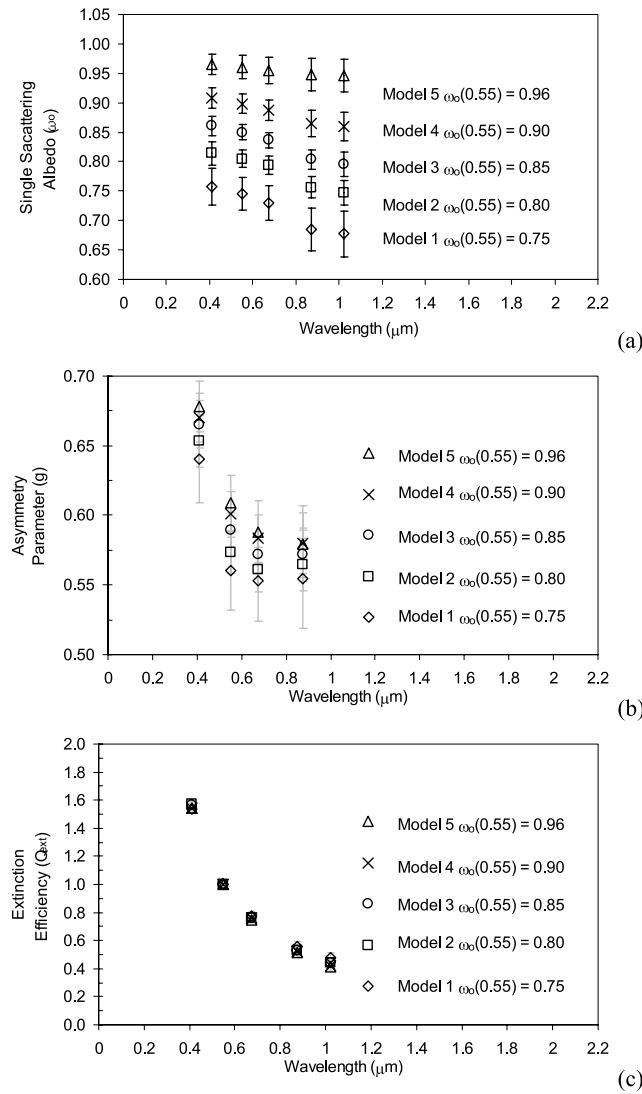


**Figure 2.** Spectral optical properties of aerosol models defined as function of wavelength. Symbols represent the aerosol properties defined based on CIMEL/AERONET measurements located in the São Paulo urban area, 2002–2003. (a) Spectral single scattering albedo ( $\omega_o$ ) and corresponding standard deviation; (b) Asymmetry parameter ( $g$ ) with standard deviation around 0.04 at 0.67; (c) Extinction efficiency ( $Q_{\text{ext}}$ ) with standard deviation around 0.02 at 0.67.

different kinds of surfaces, *Kaufman et al.* [1997c] presented a mean relationship of  $\rho_{\text{surf}}(0.65) = \rho_{\text{surf}}(2.1) \cdot 0.50$  that was used in the MODIS retrieval collection 4. Recent studies using the AERONET database to correct the atmospheric effect show that the average ratio between  $\rho_{\text{surf}}(0.65)$  and  $\rho_{\text{surf}}(2.1)$  is closer to 0.56 in a global sense [*Levy et al.*, 2007]. The authors show that this factor is also a function of the surface vegetation index and scattering angle. An updated surface parameterization has been recently applied to a new MODIS algorithm, Collection 5. *Levy et al.* [2007] show that over urban areas this ratio can be between 0.6 and 0.75. *Castanho et al.* [2007] have computed this ratio for Mexico City’s urbanized areas and found values around  $0.73 \pm 0.06$ . We performed simulation

analyses of different ratios of VIS/SWIR in this work from 0.5 up to 0.75. The results showed that the  $\tau_a$  retrieved has a constant positive or negative offset compared to the ground-based measurement from AERONET. A ratio of 0.6 was assumed for the region because it gave the best results in the simulation analyses.

### 4.3. Aerosol Optical Models Identified in São Paulo

[12] A high diversity of aerosol particles influence São Paulo air pollution. This variability makes retrieval of  $\tau_a$  complex. For this reason, we defined a collection of aerosol optical models that represent the heterogeneity of the aerosol over the studied region. The aerosol optical properties of the region were analyzed based on a set of 350 AERONET measurements from 2002 to 2003. Performing a cluster analysis, we identified five aerosol optical models based on the spectral single scattering albedo (at wavelengths 1.02, 0.87, 0.67, and 0.47  $\mu\text{m}$ ). The five aerosol optical models were defined by an average of the optical properties in each identified cluster. The optical properties that define an aerosol optical model are the single scattering albedo ( $\omega_o(\lambda)$ ), the phase function ( $P(\Theta, \lambda)$ ), and the extinction efficiency ( $Q_{\text{ext}}(\lambda)$ ). We used the Henyey–Greenstein approximation for the phase function, defined in terms of the asymmetry parameter ( $g(\lambda)$ ). For scattering angles between 110 and 140 degrees, the Henyey–Greenstein function represents the original phase function with maximum differences of 15%, and it was used in this study to save computation time.

[13] Figure 2 presents the  $\omega_o(\lambda)$ ,  $g(\lambda)$ , and  $Q_{\text{ext}}(\lambda)$  of the five aerosol optical models identified in the cluster analyses. The single scattering albedo varies significantly from 0.75 in Model 1 through 0.96 in Model 5 at wavelength 0.55  $\mu\text{m}$ . The new MODIS algorithm collection 5 assumes a single, but seasonally varying, aerosol model with  $\omega_o(0.55\mu\text{m}) = 0.85$  to 0.90, depending on the season and the region [*Levy et al.*, 2007], that is similar to our mean aerosol models numbers 3 and 4. Figure 2 also presents the asymmetry parameter and extinction efficiency from AERONET climatology results for Sao Paulo.

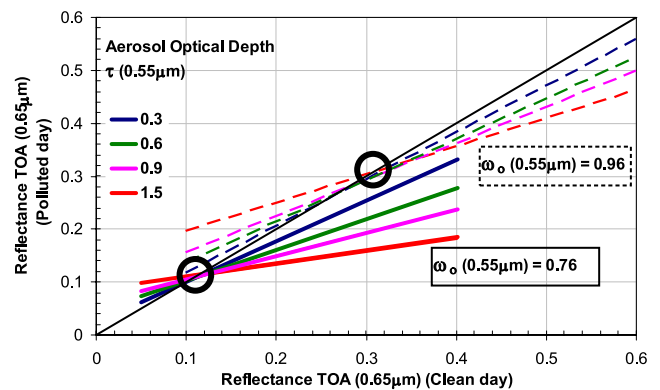


**Figure 3.** Reflectance at the top of the atmosphere (TOA) for a polluted day as a function of the reflectance at the TOA for a clean day. The group of curves represents aerosol with different single scattering albedos (0.76 and 0.96 at 0.55  $\mu\text{m}$ ) for aerosol optical depth varying from 0.3 up to 1.5.



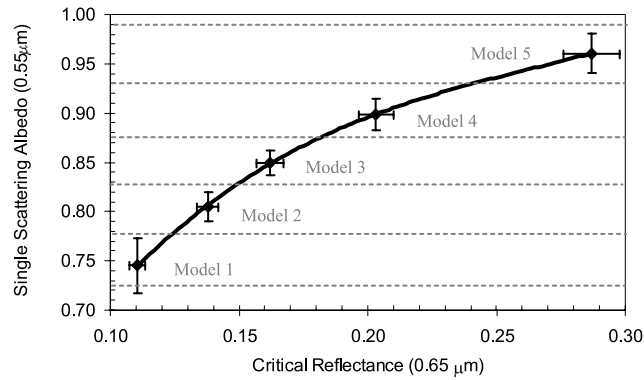


**Figure 4.** Mean and standard deviation of single scattering albedo at  $0.55 \mu\text{m}$  corresponding to each aerosol model as a function of the averaged and standard deviation of critical reflectance at  $0.65 \mu\text{m}$  simulated for different aerosol optical thicknesses. The critical reflectances were simulated using SBDART radiative transfer code for each one of the five different aerosol optical models for a given satellite and solar geometry.

#### 4.4. Description of the Dynamical Methodology of Critical Reflectance

[14] The choice of an adequate aerosol optical model is crucial in the satellite retrieval of  $\tau_a$ , as shown by the sensitivity tests. For this reason, we developed a dynamic methodology to identify the aerosol model that best represents the real aerosol characteristics. The methodology uses the critical reflectance property defined and described by *Fraser and Kaufman* [1985] as a surface property and later described by *Martins* [1999] as an intrinsic property of the aerosol particles.

[15] The reflectance measured at the top of the atmosphere ( $\rho_{\text{TOA}}$ ) can be decomposed into two terms, as shown in equation (1) as presented by *Fraser and Kaufman* [1985]. The first term exclusively represents the contribution of the reflectance of the atmosphere ( $\rho_o$ ) to the reflectance at the TOA. The reflectance due to the atmosphere is constituted by the sum of reflectance due to the gases molecules plus the aerosol layer. The second term of

equation (1) includes the contribution of the direct and diffuse transmission of radiance downward ( $T_d$ ) and upwards ( $T_s$ ) through the atmosphere that is reflected by the surface ( $\rho_{\text{Surf}}$ ). The factor  $1/(1-s\rho_{\text{Surf}})$  expresses the multiple reflections between the surface and the atmosphere; it can be neglected in most of the cases when the product ( $s\rho_{\text{Surf}}$ ) is small [*Kaufman et al.*, 1997b].

$$\rho_{\text{TOA}}(\lambda, \theta_0, \theta, \phi_o, \phi) = \rho_o(\lambda, \theta_0, \theta, \phi_o, \phi) + \frac{T_d(\lambda, \theta_0)T_s(\lambda, \theta)}{(1 - s\rho_{\text{Surf}})}\rho_{\text{SUP}}(\lambda, \theta_0, \theta, \phi_o, \phi) \quad (1)$$

[16] Where  $\lambda$  is the wavelength,  $\theta_0$  and  $\theta$  are the zenith angles and  $\phi_o$ ,  $\phi$  are the azimuth angles of the sun and the observer, respectively.

[17] *Fraser and Kaufman* [1985] presented this equation, showing that the reflectance at the TOA is linear with respect to the surface reflectance, when the  $1/(1 - s\rho_{\text{Surf}})$  is considered negligible. The authors also discuss how the balance between the two terms on the right of (1) shows that the atmospheric aerosol load can increase or decrease the reflectance at the TOA, depending on the relative properties of the aerosol single scattering albedo and the surface reflectance. In other words, if the surface reflectance is low (dark surfaces), the inclusion of aerosol could increase the reflectance at the TOA, while the same type and amount of aerosol over a bright surface could reduce the reflectance at the top of the atmosphere. There exists, therefore, a surface reflectance value in between these conditions for which the aerosol loading does not change the reflectance at the top of the atmosphere, called the critical reflectance. As performed by *Martins* [1999], combining (1) for the cases of a polluted and a clean day, yields equation (2), when considering the factor  $1/(1 - s\rho_{\text{Surf}})$  negligible.

$$\rho_{\text{TOA}}^{\text{Polluted}} = (\rho_{\text{OPol}} - \rho_{\text{OClean}})A + \rho_{\text{TOA}}^{\text{Clean}}B \quad (2)$$

$$B = \frac{T_d^{\text{Pol}}T_s^{\text{Pol}}}{T_d^{\text{Clean}}T_s^{\text{Clean}}}$$

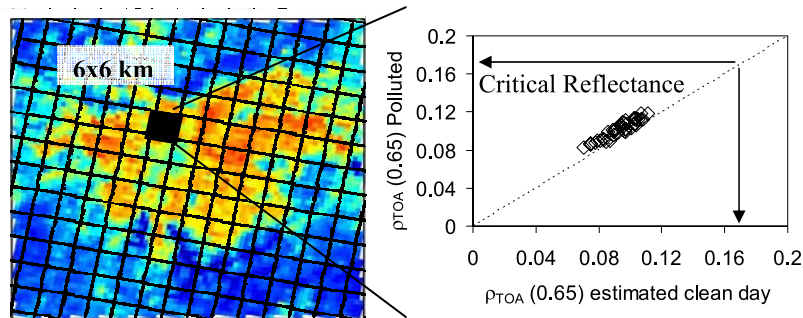


**Figure 5.** (a) Illustration of São Paulo metropolitan area divided into sub-areas of  $6 \times 6 \text{ km}$ . (b) The regression in one of the sub-areas of the reflectance at the TOA ( $\rho_{\text{TOA}}(0.65)$ ) for a polluted day as function of the  $\rho_{\text{TOA}}$  estimated for  $\tau_a = 0$  based on the estimated surface reflectance at  $0.65 \mu\text{m}$ .

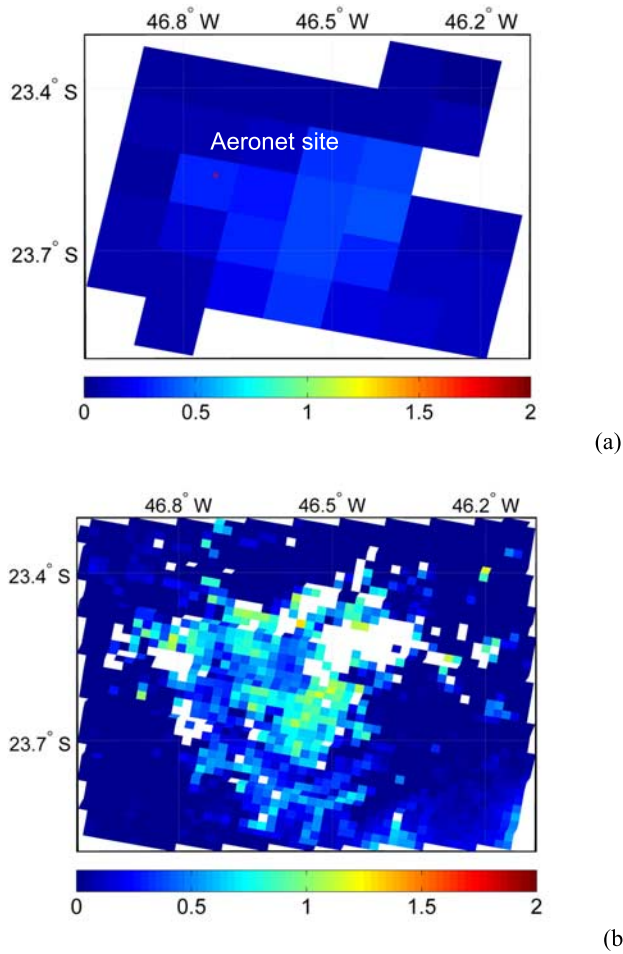


**Figure 6.** Aerosol optical depth retrievals for a polluted day on 22 August 2000, at 10:30AM using MODIS on the Terra satellite. (a) Aerosol optical depth  $\tau_a$  ( $0.55 \mu\text{m}$ ) over the São Paulo metropolitan area with 10 km spatial resolution from MODIS operational product (Collection 5); (b) Aerosol optical depth  $\tau_a$  ( $0.55 \mu\text{m}$ ) retrieved over São Paulo metropolitan area with 1.5 km spatial resolution in this work. The critical reflectance dynamical methodology was used here to identify the aerosol model to be used in the retrieval. The mean aerosol model #3 was considered over the regions where the critical reflectance could not be identified.

where the critical reflectance of a aerosol type can be expressed as

$$\rho_C = \frac{(\rho_{OPol} - \rho_{OClean} \cdot B)}{(1 - B)} \quad (3)$$

[18] Note that the critical reflectance is a function only of the atmospheric optical properties.

[19] The contribution of the aerosol optical depth to the reflectance at the TOA on a polluted day compared to a clean day as defined in (2) can be well visualized as shown in Figure 3. We simulated, using the radiative transfer code SBDART, the reflectance at the TOA for a polluted day and for a clean day, considering surface reflectance varying from

0 up to 0.6, with a fixed geometry of the observer and the sun. The polluted conditions were simulated by two cases, in which an aerosol layer with single scattering albedo of 0.76 and 0.96 and with optical depth varying from 0.3 up to 1.5 were used.

[20] Figure 3 shows the linearity between the  $\rho_{TOA}$  in the polluted and clean days. The group of curves with the same  $\varpi_o$  and with different aerosol optical depths intercept at one point. The reflectance corresponding to the intersection point represents the critical reflectance, defined in equation (3). In other words, we can define the critical reflectance as the reflectance at the top of the atmosphere that is invariant with the aerosol optical depth. It is directly related to the aerosol single scattering albedo as shown in Figure 4.

[21] Figure 4 shows the relation between the critical reflectance and different  $\varpi_o$  corresponding to the five aerosol models defined in this work for a given satellite and solar geometry. On the basis of this relationship, once the collection of aerosol models for the São Paulo region

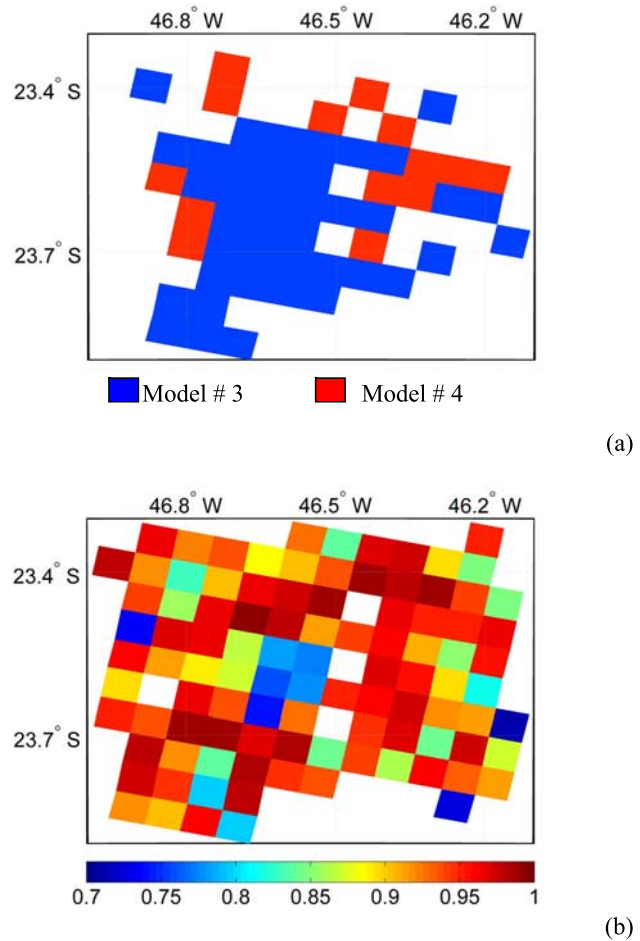


**Figure 7.** Dynamic aerosol model methodology sub-products, for 22 August 2000, at 10:30AM retrieved from MODIS on the Terra satellite: (a) derived aerosol models from the critical reflectance dynamic methodology analyses. (b) Squared correlation coefficient ( $r^2$ ) from the linear fit of the critical reflectance retrieval representing each sub area of  $6 \times 6 \text{ km}$ . The regions where the  $r^2$  were lower than 0.7 appear in white.

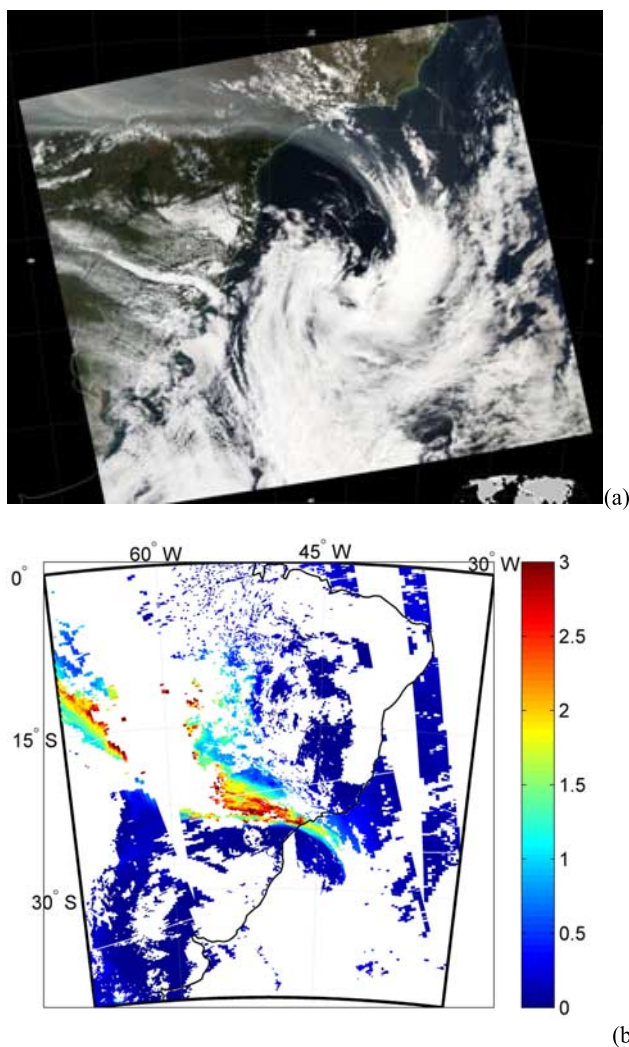


**Figure 8.** Case study of long range transport of biomass burning aerosols from Amazônia passing over São Paulo on 15 September 2004. (a) Visible composition image (from MODIS reflectance <http://modis-atmos.gsfc.nasa.gov/IMAGES/index.html>). (b) Aerosol optical depth retrieved from MODIS operational product at  $0.55 \mu\text{m}$  with 10 km resolution.

was defined as a function of  $\varpi_o$ , determining the critical reflectance with the MODIS sensor implies determining the aerosol model. The critical reflectance estimated from MODIS can be derived independently of any assumption of the aerosol model, with sufficient time resolution (for each day) and spatial resolution (at least  $6 \times 6 \text{ km}$ ) over the studied area to allow a dynamical determination of the aerosol model in the retrieval of  $\tau_a$ .

[22] The computation of the critical reflectance with the satellite data was performed over sub-areas of  $6 \times 6 \text{ km}$ . For each of these sub-areas, we calculated a linear regression between the reflectance measured at TOA at  $0.65 \mu\text{m}$  (1.5 km) and the estimated reflectance at the TOA at  $0.65 \mu\text{m}$  for  $\tau_a$  equal to zero to represent a clean day, as Figure 5 shows. We estimate the reflectance at the top of the atmosphere for  $\tau_a = 0$  based on the estimated surface reflectance at  $0.65 \mu\text{m}$  using the surface reflectance ratios discussed in

section 4.2. We obtain a regression curve like the one exemplified in Figure 5b for each single sub-area. The regression provides the critical reflectance, which is related to an aerosol model, as Figure 5 shows.

[23] The critical reflectance can be well defined only in regions with high surface reflectance variability and with a homogeneous aerosol layer in the analyzed area ( $6 \times 6 \text{ km}$  in this case). To assure the quality of the information, we considered only critical reflectances with a correlation coefficient ( $r^2$ ) greater than 0.7. The other important issue is that the critical reflectance has been defined based on

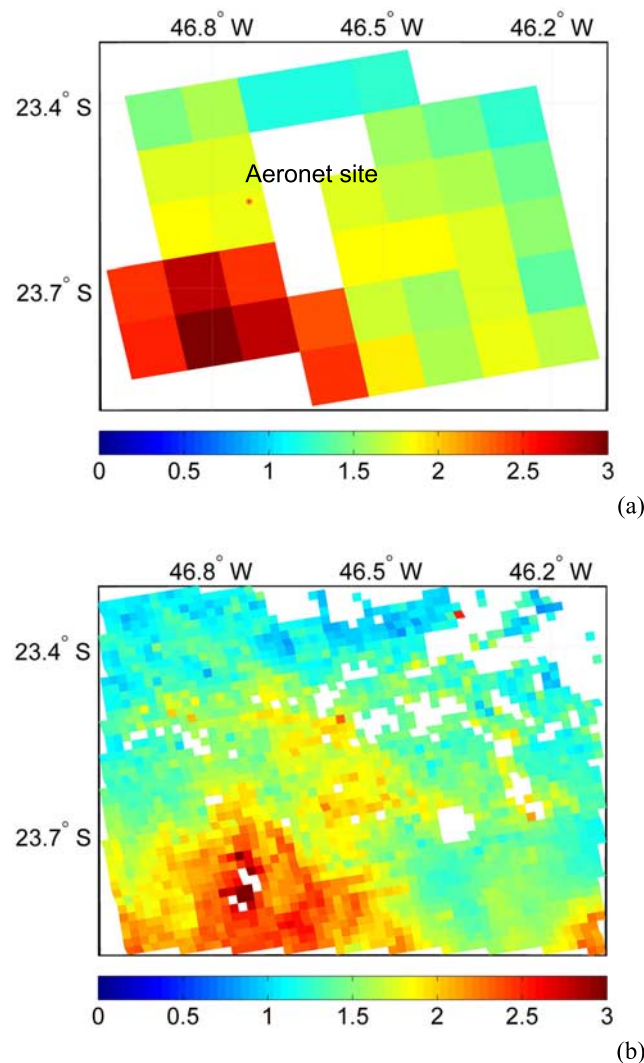


**Figure 9.** Approximated image over the São Paulo urban area showing MODIS retrievals (15 September 2004, at 1:30PM using MODIS on the Aqua satellite). (a) Aerosol optical depth  $\tau_a$  ( $0.55 \mu\text{m}$ ) over the São Paulo metropolitan area with 10 km spatial resolution from the MODIS operational product (Collection 5); (b) Aerosol optical depth  $\tau_a$  ( $0.55 \mu\text{m}$ ) retrieved over the São Paulo metropolitan area with 1.5 km spatial resolution using the critical reflectance dynamical methodology. Over the regions where the critical reflectance could not be identified, the dominant aerosol model #4 was used.



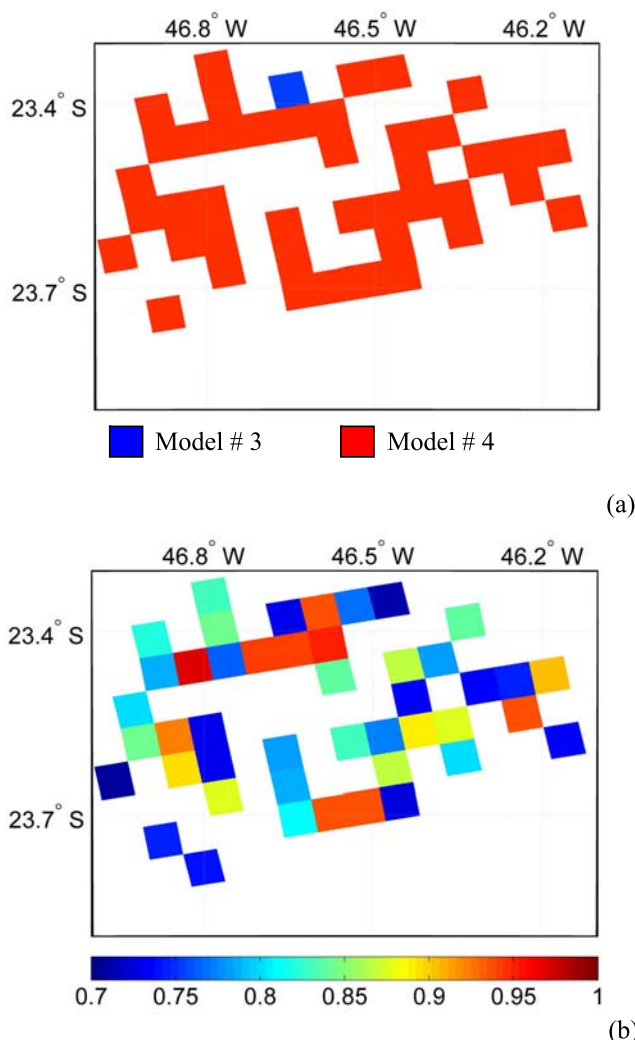


**Figure 10.** Results of the dynamic aerosol model methodology for 15 September 2004, at 10:30 AM using MODIS on the Terra satellite: (a) Identified aerosol model from the dynamical methodology (between aerosol model 3 and 4); (b) Square correlation coefficient ( $r^2$ ) from the linear fit of the critical reflectance retrieval, representing each sub area of  $6 \times 6$  km. The regions where the  $r^2$  values were lower than 0.7 appear in white.

the assumed surface reflectance. The surface reflectance in the visible wavelength is estimated based on a ratio between the visible and shortwave infrared reflectances, as described in section 4.2. This ratio can vary depending on the surface type and scattering angle but not sufficiently to affect the critical reflectance in the urban area with the resolution we are proposing here. On the basis of these uncertainties, we reduced the resolution of the critical reflectance using only two of the five aerosol models in this work. The two aerosol models on average represent models with low (aerosol model 3,  $\omega_o = 0.85$ ) and high (aerosol model 4,  $\omega_o = 0.90$ ) single scattering albedo. More accurate surface reflectance information is essential to improve the resolution of the critical reflectance property and should be further analyzed.

#### 4.5. Building Inversion Equations

[24] The inversion equations relate a simulated reflectance at the top of the atmosphere to a given aerosol optical depth for a specific surface reflectance, aerosol optical model, and solar and sensor geometry. The inversion equations were generated with the SBDART radiative transfer code, which was run for all combinations of the listed variables.

[25] We studied the area between latitude  $-23.9^\circ$  to  $-23.3^\circ$  and longitude  $-47.0^\circ$  to  $-46.1^\circ$ . Spectral solar irradiance values were extracted from the Lowtran-7 model available in the SBDART library. The atmospheric water vapor amount was based on the measurements of the AERONET instrument for the day of interest and averaged over a time period of 2 h around the satellite overpass time. The average surface pressure was assumed to be 935 mb based on local measurements. We assumed the tropical region climatologic temperature and gas profiles from the SBDART library. The sensor and solar geometry used was an average of the angular positions over the specified region (less than one degree) for each day of study, which is an approximation that does not significantly affect the  $\tau_a$  product. A collection of inversion equations was generated for each geometry, aerosol optical model, and surface reflectance. Figure 1 illustrates all the combinations for which the inversion equations were constructed.

[26] We computed a polynomial regression of degree 3 that fit the  $\tau_a$  as a function of the reflectance at the TOA simulated for each one of the above conditions. The equations that presented  $r^2$  correlation coefficients smaller than 0.96 were considered inappropriate for use in the retrieval of  $\tau_a$ . This low correlation occurs in conditions where there was very little variation in the reflectance at the TOA for a large range of  $\tau_a$ , or in other words, near-critical reflectance conditions. These situations were avoided to increase the quality of the retrieval of  $\tau_a$  from MODIS.

## 5. Results and Discussions

### 5.1. Case Studies: Local and Long Range Transport of Pollution

[27] Aerosol properties can change from one day to another. As an example, we present here a case study dominated by local pollution and then another one strongly affected by the transport of aerosols from biomass burning in Amazônia to the São Paulo region.

[28] Figure 6 shows the  $\tau_a$  at  $0.55 \mu\text{m}$  retrieved for 22 August 2000, representing a high local aerosol optical depth, reaching 1.0 in some regions. Figure 6a presents the AOD product with 10 km spatial resolution from MODIS standard product, and Figure 6b presents the AOD product from this work with 1.5 km spatial resolution. The in situ ground-based network (data from the local Environmental Protection Agency - CETESB) measured  $\text{PM}_{10}$  concentrations that ranged from 80 up to  $180 \mu\text{g m}^{-3}$  on this day at the time around the satellite overpass. It is interesting to note the high aerosol loading confined to the urbanized area in this case, showing that it is a local plume and not transported from other regions. The white pixels in the image may be clouds and were removed from the analyses during the quality assurance step. Other pixels removed during quality assurance include cases near the critical



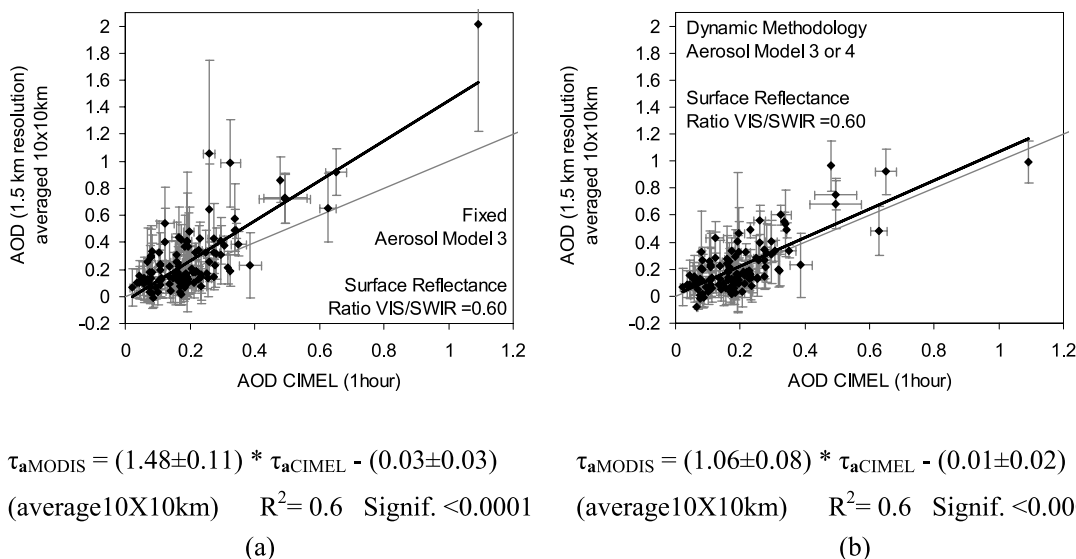


**Figure 11.** Aerosol optical depth  $\tau_a$  ( $0.55 \mu\text{m}$ ) product retrieved from MODIS in this work over São Paulo compared to AERONET (black symbols) collocated in space and time. MODIS retrieval with 1.5 km resolution was averaged over  $10 \times 10$  km around each measurement site and compared to 1 h averages of the ground-based data. Surface reflectance was estimated using the relation ( $\rho_{\text{surf}}(0.65) = 0.60 * \rho_{\text{surf}}(2.1)$ ). (a) MODIS  $\tau_a$  ( $0.55 \mu\text{m}$ ) retrieved using a constant aerosol model (#3) for all days; (b) MODIS  $\tau_a$  ( $0.55 \mu\text{m}$ ) retrieved using the dynamic methodology developed in this study, which identifies the better of the two aerosol models with single scattering albedos 0.85 and 0.90. The linear regression is denoted in the figure with the solid line; the dotted line denotes the 1:1 line. The regression equation is given at the bottom of each figure.

reflectance. Figure 7a presents the aerosol model identified by the dynamic methodology in each sub area of  $6 \times 6$  km. Note that most of the identified aerosol was model 3.

[29] An episode of transport of biomass-burning pollution from Amazônia through the São Paulo urban area occurred on 15 September 2004. The  $\tau_a$  measured by the AERONET sun/sky radiometer reached 10 times the mean São Paulo  $\tau_a$  measurements of 0.2, while aerosol mass concentration ( $\text{PM}_{10}$ ) measured from the ground showed relatively low values ranging from 40 up to  $70 \mu\text{g m}^{-3}$  (CETESB). The relatively low mass concentrations measured from the ground as compared to the high values of  $\tau_a$  occur because the biomass-burning plume is transported above the mixing layer, and it does not influence the ground level concentrations. Figure 8a shows the MODIS RGB composite image of this plume. Figure 8b presents the operational MODIS aerosol  $\tau_a$  product (Level 2) with 10 km resolution for most of Brazil. The distribution pattern of the plume can be observed over the South Eastern part of Brazil with  $\tau_a$  ranging from 1 to 3. Figure 9 presents a close-up view over the São Paulo urban area of the  $\tau_a$  retrieved from the MODIS operational products ( $10 \times 10$  km) and the  $\tau_a$  retrieved in this work ( $1.5 \times 1.5$  km) using the dynamic critical reflectance methodology. The increase in the resolution of the  $\tau_a$  to 1.5 km shows a detailed distribution of the plume over the urban area and vicinities, with a maximum to the SW, as shown in the MODIS operational product.

[30] Figure 10a presents the aerosol model identified by the dynamical methodology and Figure 10b shows the results of the  $r^2$  coefficient obtained for each  $6 \times 6$  km

sub area. The retrieved aerosol model shows that the dominant aerosol of this day is best represented by the aerosol model 4 and not 3. This aerosol model has a single scattering albedo around 0.9 that is higher than that observed for the local pollution (0.85) and is very close to the single scattering albedo observed for biomass-burning aerosol measured locally in Amazonia [Procópio *et al.*, 2003; Remer and Kaufman, 1998] around 0.9. The dynamic algorithm developed here automatically identified an accurate aerosol model over the region. These two case studies show the importance and flexibility of the proposed methodology for the semi-real time identification of a more accurate aerosol model to be used in the retrieval of the  $\tau_a$  via satellite.

[31] An important point to be emphasized is that the difference between the urban and the biomass burning aerosol was large enough to be identified by the critical reflectance technique. As was shown in the sensitivity study, the aerosol model plays an important role in the retrieval of  $\tau_a$ , and the use of the critical reflectance technique showed significant potential to discern between the two main aerosol types. Further analysis of the surface reflectance ratio over urban areas could increase the accuracy even further.

## 5.2. Validation Comparison

[32] To test the consistency of the methodology, we compared the  $\tau_a$  produced from MODIS and the one measured from AERONET, considering data from 2002 until 2005. The methodology used in the comparison was the same as that described by Ichoku *et al.* [2002]. We

compared the AOD retrieved from MODIS with 1.5 km resolution averaged in the  $\sim 10 \times 10$  km area around the AERONET site in Sao Paulo city with the 1-h average of the AERONET data obtained around the satellite overpass time.

[33] The comparison between the retrieved AOD from satellite and the one measured by AERONET showed a lower correlation when all five aerosol models were included. The possible reason for this may be because of the uncertainties on the surface reflectance, resulting in an inaccurate result of the critical reflectance. Thus we restricted the options to 2 aerosol models: aerosol model #3 ( $\varpi_o = 0.85$ ) and aerosol model #4 ( $\varpi_o = 0.90$ ). The comparisons of the AOD are shown in Figure 11.

[34] We considered as a first simulation a fixed aerosol model (model #3) on the  $\tau_a$  retrieval; the result is presented in Figure 11a. Although model #3 is a good mean aerosol model for the region, it cannot represent all of the aerosol on every day of the retrieval, as it tends to overestimate  $\tau_a$  in some of the cases. Figure 11b shows the comparison when the dynamic methodology is applied, including two aerosol models. The results of the comparison show that some of the retrievals better match the AERONET data when aerosol model #4 is used. Some episodes of aerosol pollution in Sao Paulo are due to the transport of biomass burning from Amazonia to the region, changing significantly the aerosol optical properties during these events. The average model, represented by model #3 in the simulation shown in Figure 11a, fails to explain the optical properties of these biomass burning aerosol events. On the other hand, the new dynamic algorithm (Figure 11b) proposed here provides an effective way to identify an appropriate aerosol model to better represent the real aerosol in the atmosphere. The biomass burning case is a good example of this approach over Sao Paulo.

## 6. Summary and Conclusions

[35] Sensitivity studies show that the quality of the aerosol optical depth retrieved by satellite is directly related to the accuracy of the assumed aerosol optical property, and to the assumed surface reflectance. In this work we developed an algorithm to retrieve aerosol optical depth with high spatial resolution from MODIS radiances using local properties of the aerosol and surface characteristics. We developed a dynamic methodology using aerosol critical reflectance to reduce uncertainties in the AOD product due to uncertainties in the aerosol optical properties. The methodology uses the critical reflectance estimated from sensor data to identify the best assumption for single scattering albedo. The case studies of the local pollution and long range transport of biomass burning show the potential of the developed methodology to automatically identify the aerosol optical model, by their successful selection of two different aerosol optical models for the region: urban ( $\varpi_o = 0.85$ ) and biomass burning ( $\varpi_o = 0.90$ ). Surface reflectance issues over urban areas still require further study. In this work we used the estimated ratio of 0.6 between the visible and shortwave near infrared wavelength. Improving urban surface characterization could increase the accuracy of the results presented here. In general, this methodology was able to distinguish the  $\varpi_o$

from two different aerosol plumes using satellite based measurements over the Sao Paulo region, which is an improvement over making an a priori assumption of fixed aerosol optical properties. The surface reflectance is an important issue and needs to be better estimated to allow the use of more aerosol optical models in the dynamic methodology.

[36] The applicability of the dynamic methodology based on critical reflectance to other urban areas, as well as globally, is worth further investigation. There are two main issues to be careful of when applying this methodology to other regions: the aerosol optical models and the accuracy of the surface reflectance estimation. In addition to the single scattering albedo, the phase function of the aerosol varies significantly around the globe and needs to be taken into account. The ratio between visible to shortwave infrared is important information for this algorithm. It was locally identified for the Sao Paulo region. Further analyses should be performed to better understand the relation between this ratio and other indices in order to estimate it in an operational way. Implementation of this dynamic methodology to other areas is both important and promising.

[37] **Acknowledgments.** We thank the AERONET site managers for establishing and maintaining CIMEL instrument in Sao Paulo. We thank the reviewers for their valuable comments and contributions. We thank Matthew Alvarado for the important help on the English edition of this manuscript. This research had financial support from FAPESP 99/12493-2. J. Vanderlei Martins was partially funded by the MODIS aerosol group and by the NASA Radiation Science Program grant RSP-0269-0154.

## References

- Artaxo, P., J. V. Martins, M. A. Yamasoe, A. S. Procopio, T. M. Pauliquevis, M. O. Andreae, P. Guyon, L. V. Gatti, and A. M. C. Leal (2002), Physical and chemical properties of aerosols in the wet and dry season in Rondônia, Amazonia, *J. Geophys. Res.*, *107*(D20), 8081, doi:10.1029/2001JD000666.
- Castanho, A. D. A., and P. Artaxo (2001), São Paulo aerosol source apportionment for wintertime and summertime, *Atmos. Environ.*, *35*, 4889–4902.
- Castanho, A. D. A., R. Prinn, V. Martins, C. Ichoku, M. Herold, L. Molina (2007), Urban Visible/SWIR surface reflectance ratios from satellite and sun photometer measurements in Mexico City, ACPD, submitted for publication.
- Chu, D. A., Y. J. Kaufman, G. Zibordi, J. D. Chern, J. Mao, C. Li, and B. N. Holben (2003), Global monitoring of air pollution over land from the Earth Observing System-Terra Moderate Resolution Imaging Spectroradiometer (MODIS), *J. Geophys. Res.*, *108*(D21), 4661, doi:10.1029/2002JD003179.
- Dubovik, O., and M. D. King (2000), A flexible inversion algorithm for retrieval of aerosol optical properties from sun and sky radiance measurements, *J. Geophys. Res.*, *105*(D16), 20,673–20,696.
- Fraser, R., and Y. J. Kaufman (1985), The relative importance of aerosol scattering and absorption in remote sensing, *Trans. Geosci. Remote Sens.*, *GE-23*(5), 625–633.
- Freitas, S., K. Longo, M. Silva Dias, P. Silva Dias, R. Chatfield, E. Prins, P. Artaxo, G. Grell, and F. Recuero (2005), Monitoring the transport of biomass burning emissions in South America, *Environ. Fluid Mech.*, *5*(1–2), 135–167.
- Holben, B. N., D. Tanré, A. Smirnov, T. F. Eck, I. Slutsker, N. Abuhassan, W. W. Newcomb, J. S. Schafer, et al. (2001), An emerging ground-based aerosol climatology: Aerosol optical depth from AERONET, *J. Geophys. Res.*, *106*(D11), 12,067–12,097.
- Ichoku, C., D. A. Chu, S. Mattoo, Y. J. Kaufman, L. A. Remer, D. Tanré, I. Slutsker, and B. N. Holben (2002), A spatiotemporal approach for global validation and analysis of MODIS aerosol products, *Geophys. Res. Lett.*, *29*(12), 8006, doi:10.1029/2001GL013206.
- Kaufman, Y. J. (1987), Satellite sensing of aerosol absorption, *J. Geophys. Res.*, *92*(D4), 4307–4317.
- Kaufman, Y. J., D. Tanré, L. A. Remer, E. F. Vermote, A. Chu, and B. N. Holben (1997a), Operational remote sensing of tropospheric aerosol over

- land from EOS moderate resolution imaging spectroradiometer, *J. Geophys. Res.*, *102*(D14), 17,051–17,067.
- Kaufman, Y. J., D. Tanre, H. R. Gordon, Nakajima, J. Lenoble, R. Frouin, H. Brassl, B. M. Herman, M. D. King, and P. M. Teillet (1997b), Passive remote sensing of tropospheric aerosol and atmospheric correction for the aerosol effect, *J. Geophys. Res.*, *102*(D14), 16,815–16,830.
- Kaufman, Y. J., A. E. Wald, L. A. Remer, B. C. Gao, R. R. Li, and L. Flynn (1997c), The MODIS 2.1  $\mu\text{m}$  Channel – Correlation with visible reflectance for use in remote sensing of aerosol, *IEEE Trans. Geosci. Remote Sens.*, *35*(5), 1286–1298.
- Kaufman, Y. J., N. Gobron, B. Pinty, J. Widlowski, and M. M. Verstraete (2002), Relationship between surface reflectance in the visible and mid-IR used in MODIS aerosol algorithm—Theory, *Geophys. Res. Lett.*, *29*(23), 2116, doi:10.1029/2001GL014492.
- King, M. D., W. P. Menzel, Y. J. Kaufman, D. Tanré, B. C. Gao, S. Platnick, S. A. Ackerman, L. A. Remer, R. Pincus, and P. A. Hubanks (2003), Cloud and aerosol properties, precipitable water, and profiles of temperature and water vapor from MODIS, *IEEE Trans. Geosci. Remote Sens.*, *41*(2), 442–458.
- Levy, R. C., L. A. Remer, S. Matto, E. F. Vermote, and Y. J. Kaufman (2007), Second-generation operational algorithm: Retrieval of aerosol properties over land from inversion of Moderate Resolution Imaging Spectroradiometer spectral reflectance, *J. Geophys. Res.*, *112*, D13211, doi:10.1029/2006JD007811.
- Li, C., A. K. H. Lau, J. Mao, and A. Chu (2005), Retrieval, validation, and application of the 1-km aerosol optical depth from MODIS measurements over Hong Kong, *IEEE Trans. Geosci. Remote Sens.*, *43*(11), 2650–2658.
- Martins, J. V. (1999), O Efeito de Partículas de Aerossol de queimadas da Amazônia no balanço Radiativo da Atmosfera. São Paulo, Tese de Doutorado, Instituto de Física, USP.
- Martins, J. V., D. Tanré, L. Remer, J. Y. Kaufman, S. Mattoo, and R. Levy (2002), MODIS cloud screening for remote sensing of aerosols over ocean using spatial variability, *Geophys. Res. Lett.*, *29*(12), 8009, doi:10.1029/2001GL013252.
- Parkinson, C. L. (2003), Aqua: An Earth-observing satellite mission to examine water and other climate variables, *IEEE Trans. Geosci. Remote Sens.*, *41*(2), 173–183.
- Procópio, A., L. A. Remer, P. Artaxo, Y. J. Kaufman, and B. N. Holben (2003), Modeled spectral optical properties for smoke aerosols in Amazonia, *Geophys. Res. Lett.*, *30*(24), 2265, doi:10.1029/2003GL018063.
- Remer, L. A., and Y. J. Kaufman (1998), Dynamic aerosol model: Urban/industrial aerosol, *J. Geophys. Res.*, *103*, 13,859–13,871.
- Remer, L. A., Y. J. Kaufman, D. Tanre, S. Mattoo, D. A. Chu, J. V. Martins, et al., (2005), The MODIS aerosol algorithm, products, and validation, *J. Atmos. Sci.-Special Edition*, *62*, 947–973.
- Ricchiazzi, P., S. Yang, C. Gautier, and D. Sowle (1998), SBDART: A research and teaching software tool for plane-parallel radiative transfer in the Earth's atmosphere, *Bull. Am. Meteorol. Soc.*, *79*, 2101–2114.

---

A. D. de Almeida Castanho, Massachusetts Institute of Technology, EAPS, 77 Massachusetts Ave., B54-1411 Cambridge, MA 02139, USA. (castanho@mit.edu)

P. Artaxo, University of São Paulo, Brazil.

J. Vanderlei Martins, JCET, University of Maryland Baltimore County, and NASA/Goddard Space Flight Center, USA.